ILASS–Europe 2022, 31th Conference on Liquid Atomization and Spray Systems, 6-8 September 2022, Virtual, Israel

Predictive Modelling of Droplet-Size Distribution from Two-Fluid Spray Atomizers via Maximization of Entropy Generation

Leander Vinzenz Mehlis*[1,2], Jens Bartsch[1], Werner Hoheisel[2], Patrick Kranz[3], Markus Thommes[1]
[1]Laboratory of Solids Processing, TU Dortmund, Dortmund 44227, Germany
[2]Formulation Technology, Invite GmbH, 51061, Cologne, Germany
[3]Process Modelling and Design, Bayer AG, Leverkusen 51373, Germany
*Corresponding author: professors.fsv.bci@tu-dortmund.de, mehlis@invite-research.com

Abstract
A major challenge in spray modelling is the prediction of droplet-size distribution. In spray modelling, instead of simulating the droplet-size distribution, distributions are either fitted or substituted by a single droplet-size. Therefore, a predictive model for the simulation of the droplet-size distribution generated by two-fluid spray atomizers has been developed and validated. The model combines a semi-mechanistic approach for the prediction of the Sauter-mean diameter with a maximization of entropy generation model. A simplification of the initial approach is achieved by applying a log-normal distribution. Due to the prediction of Sauter-mean diameter, the number of optimization variables is reduced to the distribution parameter as the only variable. In addition, the model requires material attributes, two nozzle specific calibration parameters and one entropy balancing variable. For model validation liquid spray medium, liquid mass-flow rate and atomization gas pressure was studied systematically. The outlined model offers computationally cheap predictions of droplet-size distributions.

Keywords
Modelling; Spray; Maximum-entropy; Droplet-size; Two-fluid nozzle;

Introduction

Simulation of pharmaceutical formulation processes like spray drying, tablet coating and fluidized bed granulation are affected by the generated spray droplet-size distribution [1-4]. For process simulations the prediction of droplet-size is generally reduced to the prediction of a single representative droplet-size or a fitted size distribution. Several predictive models for Sauter-mean diameter (D_{32}) like Master [5] or Aliseda et al. [6] exist in scientific literature. Semi-empirical models based on instability analysis integrate the influence of process parameters and material attributes [6]. However, information on the droplet-size distribution is usually not considered.

Simulations that consider droplet-size distributions using frequently probability distribution based on to experimental data. Commonly applied distribution functions are Rosin-Rammler, Nukiyama-Tanasawa or log-normal distributions [7]. This approach either ignores the influence of changing process parameters on the spray distribution or results in excessive experimental effort.

The initial droplet size and velocity distribution can be predicted numerically by maximum entropy formalism (MEF). R. Sellens and T. Brzustowski showed the droplet-size distribution can be calculated independently from the velocity distribution [8]. The MEF approach relies on solving a constrained optimization problem and the volumetric mean droplet size. Due to the constrained optimization this approach is primary applied for complex simulations. For the prediction of droplet-size distributions Li et al. [9, 10] derived a maximization of entropy

generation (MEG) model by combining the MEF model with the second law of thermodynamics.

The aim of the study is to develop a semi-mechanistic model for the prediction of droplet-size distributions for two-fluid nozzles. Therefore, a two-parametric probability distribution was postulated to a MEG model. This reduces the computational cost of the MEG model and enables the model to be used for large sensitivity analysis. The model dependency on mean diameters can be eliminated by combination with a predictive model for Sauter-mean diameter.

Theoretical Framework

Modelling Droplet Size

The applied semi-mechanistic Aliseda model is developed for circular two fluid nozzles with external mixing [6] and is presented in eq. (1)

$$\frac{D_{32}}{D_l} = C_1(1+m_r)\left(\frac{b_g}{D_l}\right)^{1/2}\left(\frac{\rho_l/\rho_g}{Re}\right)^{1/4}\frac{1}{\sqrt{We}} \cdot\left\{1+C_2\left(\frac{D_l}{b_g}\right)^{1/6}\left(\frac{Re}{\rho_l/\rho_g}\right)^{1/12} We^{1/6}Oh^{2/3}\right\} \quad (1)$$

where D_l is the liquid orifice diameter, b_g is the boundary layer thickness, and m_r is the mass-flux ratio. Densities are given by ρ with indices g and l for gas and liquid phase, respectively. Dimensionless numbers Oh, Re, and We are the Ohnesorge, Reynolds, and Weber number, respectively [6]. The nozzle specific calibration parameters C_1 and C_2 tend to converge towards one at close proximity to the nozzle [11].

Two-fluid nozzle geometric specifications required for the Aliseda model and the corresponding spray break-up are presented in Figure 1. Spray break-up occurs in two stages. First the liquid spray breaks up into ligaments which then further break-up into droplets. According to the maximum entropy formalism the fluid at the nozzle exit is imagined as a single large droplet that breaks into the initial droplet-size distribution towards the end of the 2. breakup region. The breakage process via the spray model finishes at a critical distance x_{crit} from the nozzle. This distance can be approximated [12].

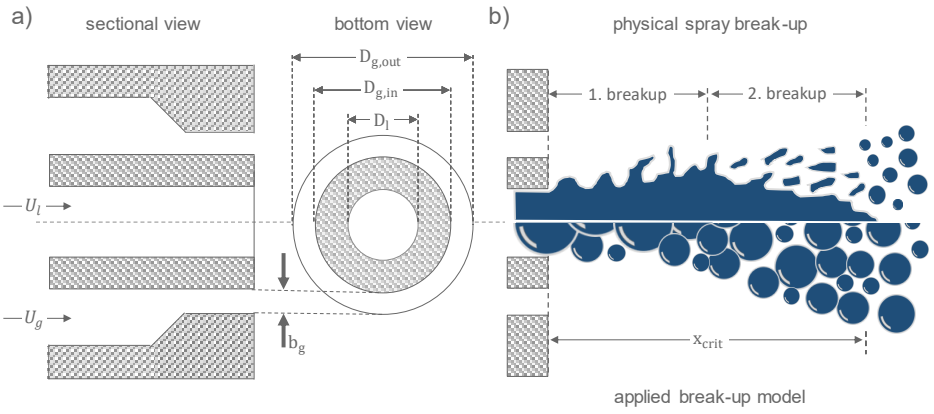

Figure **1**. Illustration of geometric specifications of a two-fluid external mixing nozzle a) and generation of initial droplet-size distribution b). Liquid and gas velocities are represented by U_l and Ug,

respectively. The boundary layer thickness b_g is the difference of the outer $D_{g,out}$ and inner $D_{g,in}$ gas ring gap diameters. At a distance x_{crit} from the nozzle the 2. breakup is concluded. Spray break-up into ligaments at 1. breakup is ignored in this model.

Modelling Droplet Size Distribution

For the prediction of the droplet-size distribution, the MEG model [9, 10] is applied. Eq. (*2*) shows the prediction of the generated mass-specific entropy s_{gen}. The right hand side of the equation shows a combination of the Shannon entropy [13] with the Gibb's equation for free interfaces [14].

$$s_{gen} = K\frac{\dot{N}_T}{\dot{m}_l}H_{sh} + ds_l \tag{2}$$

The droplet generation rate and the liquid mass flow rate are denoted by $\dot{N}_T$ and $\dot{m}_l$, respectively. The specific entropy of the liquid phase is given by s_l and K is a constant. For a specific distribution P_r the entropy is given by the Shannon entropy H_{sh} as given by eq. (*3*).

$$H_{Sh} = -\lim_{\Delta D\to 0}\sum_i P_r(D_i)\cdot ln[P_r(D_i)] \tag{3}$$

$P_r(D_i)$ is the probability of a droplet (D) of a size class i to occure. The index *r* indicates the utilised distribution type. An index of 0 or 3 refers to a number or volume-based distribution. Eq. (*4*) shows the Gibb's equation for free interfaces.

$$ds_l = \frac{\sigma_{ST}}{T}da - \frac{\kappa_T}{\rho_l T}\cdot p\, dp \tag{4}$$

where T is the temperature of the system and *a* is the specific surface area of the droplet. The isothermal compressibility κ_T and pressure *p* refer to the liquid-vapour interface [9, 10, 14]. Droplet breakage is assumed to be isothermal. Equations (3) and (4) are inserted into (2) to derive an expression for the mass-specific entropy generated [9, 10]. The generated entropy in eq. (*5*) is maximised to estimate the most probable distribution.

$$\begin{aligned} s_{gen} = & -\frac{6\,K}{\rho_l \pi D_{3,0}^3}\sum_i P_0(D_i)\cdot ln[P_0(D_i)] \\ & -\sum_i P_0(D_i)\left[\frac{8\,\sigma_{ST}\,\kappa_T}{\rho_l\,T\,D_{3,0}^2}\overline{D}_i + \frac{\sigma_{ST}\,[4\,p_1\,\kappa_T - 6]}{\rho_l\,T\,D_{3,0}}\overline{D}_i^2\right] - \frac{\sigma_{ST}}{T}a_1 \end{aligned} \tag{5}$$

A bar above the droplet diameter indicates a normalized diameter $\left(\overline{D} = D/D_{3,0}\right)$. To model the droplet-size distribution Li et al. [9, 10] applied a lagrangian form distribution on number basis to the MEG model. Fitting parameters α_i in eq. (6) need to be determined by constrained optimization, which increases the computational cost of this model. These constraints generally enforce compliance with conservation laws.

$$P_{0,LaG}(\overline{D}) = 3\overline{D}^2\, exp\{-\alpha_0 - \alpha_1\overline{D} - \alpha_2\overline{D}^2 - \alpha_3\overline{D}^3\} \tag{6}$$

For a log-normal probability distribution as shown in eq. (7) all constraints proposed [9, 10] are met.

$$P_{r,LoG}(D) = \frac{1}{\sigma_{ln}\sqrt{2\pi}}\cdot\frac{1}{D}\cdot exp\left\{-\frac{1}{2}\left(\frac{ln(D)-\mu_r}{\sigma_{ln}}\right)^2\right\} \tag{7}$$

Log-normal distributions are fully specified by the location parameter μ_r and distribution parameter σ_{ln}. Applying eq. (8), All unknown mean diameters can be calculated [15].

$$D_{p,q} = exp\{\mu_0 + (p+q)\sigma_{ln}/2\} \quad (8)$$

Experimental data is often presented in the form of volumetric 10% (D_{v10}), 50% and 90% (D_{v90}) percentiles. These can be calculated utilizing eq. (9) and the standard normal distribution values $z_{r,x}$ as given in Table 1.

$$D_{r,x} = exp\{\mu_r + z_{r,x} \cdot \sigma_{ln}\} \quad (9)$$

Table 1 – Standard normal distribution values for the calculation of the 10%, 50%, 75% and 90% percentile of a log-normal distribution

	10	50	75	90
$z_{r,x}$	-1.282	0.000	0.775	1.282

Eventually, the entropy of a log-normal distribution can be calculated by eq. (10).

$$H_{Sh,LoG} = \mu_r + \frac{1}{2}\pi e \sigma_{ln}^2 \quad (10)$$

Experimental Setup

Spray experiments for model validation were performed using water. A two-fluid spray with a liquid orifice diameter of 0.71 mm, inner and outer ring gap diameters of 1.06 and 1.30 mm was utilized. Droplet-size distributions were measured by laser diffractometry with a Malvern Spraytec (Malvern Panalytical, Malvern, UK). The laser diffractometer (LD) was located at 5 cm distance from the nozzle. At closer distances the measurement produced D_{v90} values within the same order of the liquid orifice diameter. Physico-chemical properties of the liquids [6] are presented (see Table 2).

Table 2 – Properties of atomization liquids at ambient conditions used for model validation [6]. Viscosity measurement at 225 s^{-1} shear rate.

	$\rho_l\ (kg\ m^{-3})$	$\sigma_{ST}\ (N\ m^{-1})$	$\eta\ (mPa\ s)$
Water	998	0.072	0.97

Model Development and Validation

Calibration Droplet Size Model

The droplet Sauter-mean diameter model in according to Aliseda [6] requires two calibration parameters that account for the nozzle gas ring-gap geometry and the influence of physico-chemical attributes of the spray liquid on instability growth. Therefore, a number of spray experiments were performed investigating the particle-size distribution by laser diffraction. Thereby the atomizing air pressure and the liquid flow rate were varied systematically (Figure **2** a). The Aliseda model parameters (C_1 and C_2) were found to be 1.147 and 1.702, respectively.

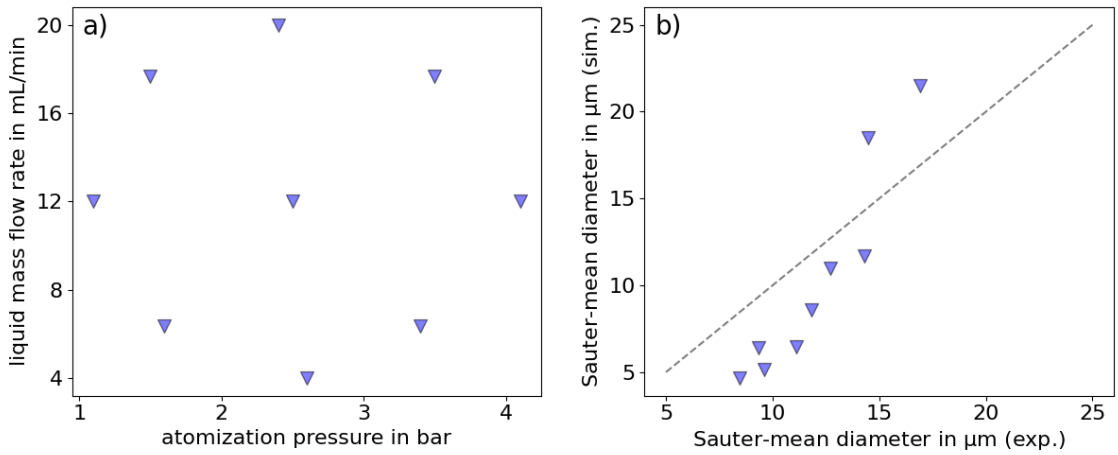

Figure **2**. Design space a) for atomization pressure and gas volumetric flowrate. Comparison of simulated and experimental values for Sauter-mean diameter b). Experiments were performed for pure water.

These parameters were used to predict the Sauter mean diameter for each individual set of operating conditions and subsequently compared to experimental data (figure 2 b). The predicted Sauter-mean diameter values are in a similar size range like the experimental data but there are systematic deviations. Firstly, the atomization pressure is a key factor for spray atomization [7] and the atomization pressure was adjusted with an uncertainty of ±0.1 bar. Applying an atomization pressure deviation of ±0.1 bar to the calibrated Aliseda model led to alterations in the predicted Sauter-mean diameter of up to ±1.9 µm. Secondly, the gas jet velocity was calculated by dividing the volumetric flow-rate by the nozzle ring-gap area. However, the calculated gas jet velocities exceeded the speed of sound. Effects caused by the gas breaking the sound barrier most probably effect the gas velocity and density.

Development Droplet Size Distribution Model

The MEG model as presented in eq. (5) is simplified by a log-normal distribution. For a log-normal distribution the normalized length based $\left(\overline{D}_{1,0}\right)$ and surface $\left(\overline{D}_{2,0}\right)$ based mean diameter are functions of the distribution parameter and can be calculated by eq. (8). The diameters $\overline{D}_{1,0}$ and $\overline{D}_{2,0}$ are linked to the droplet-size distribution via constraints postulated by Li & Li for the lagrangian form distribution [9, 10]. These constraints are presented in eq. (11*)* and (12*)*. The calculation of the normalized mean diameters for log-normal distributions avoids rounding errors and is computationally more efficient then the integration over the droplet-size distribution.

$$\int_0^\infty P_0(\overline{D}) \cdot \overline{D}\, d\overline{D} = \overline{D}_{1,0} \tag{11}$$

$$\int_0^\infty P_0(\overline{D}) \cdot \overline{D}^2\, d\overline{D} = \overline{D}_{2,0}^2 \tag{12}$$

The Shannon entropy for log-normal distributions in eq. (*10*) is applied to the MEG model in eq. (5). In addition to two calibration parameters in the Aliseda model a third calibration parameter C_3 is required. This parameter scales the Shannon Entropy to the Gibb's equation. Eventually, the simplified MEG model in eq (*13*) is a function of the volumetric mean diameter ($D_{3,0}$), log-normal distribution parameter, material properties and process parameters.

$$s_{gen} = \frac{6\,C_3}{\rho_l\,\pi\,D_{3,0}^3}\left(\bar{\mu}_0 + \frac{1}{2}ln[2\pi e\sigma_{ln}^2]\right) - \bar{D}_{1,0}\left(\frac{8\,\sigma_{ST}\,\kappa_T}{T\,\rho_l\,D_{3,0}^2}\right) - \bar{D}_{2,0}^2\left(\frac{\sigma_{ST}[4\,p_1\,\kappa_T - 6]}{T\,\rho_l\,D_{3,0}}\right) - \frac{\sigma_{ST}}{T}a_1 \qquad (13)$$

For a log-normal distribution, the normalized diameters $\bar{D}_{1,0}$ and $\bar{D}_{2,0}^2$ equal $\exp\{-\sigma_{\ln}\}$. By applying eq. (8) the volumetric mean diameter can be expressed by the Sauter-mean diameter and the distribution parameter. Therefore, in combination with a predictive model for Sauter-mean diameter maximization of entropy generation is unconstrained and only dependent of the log-normal distribution parameter.

Calibration Droplet Size Distribution Model

The calibration parameter C_3 was estimated for each individual experiment. The experimentally measured Sauter-mean diameter and volumetric 50% percentile serve as input and target value, respectively. Single values and the ensemble mean C_3 for each liquid are presented in Figure **3**.

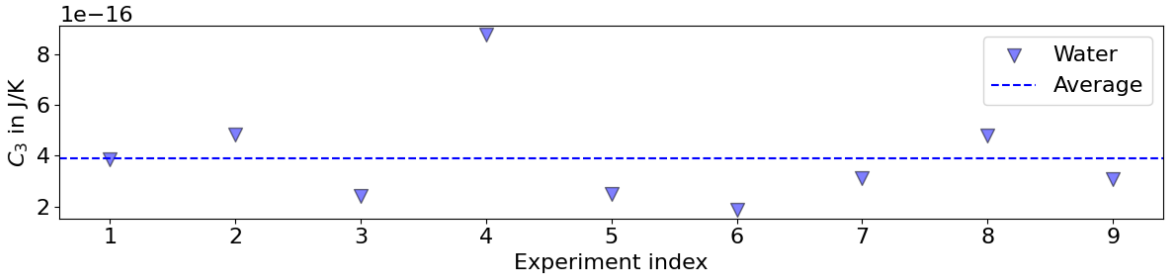

Figure **3**. Values of calibration parameter for maximization of entropy generation model for each experiment as well as an average for each liquid.

For each liquid the C_3 values are within the same order of magnitude. However, the C_3 values are scatter around an average and variations cause significant changes in the predicted D_{v10}, and D_{v90} values.

Validation Droplet Size Distribution Model

For model validation, D_{v10}, D_{v75} and D_{v90} were predicted and correlated to the measured values as shown in Figure 4. The grey dashed line indicates the potential perfect conformity of the experimental with the simulated results.

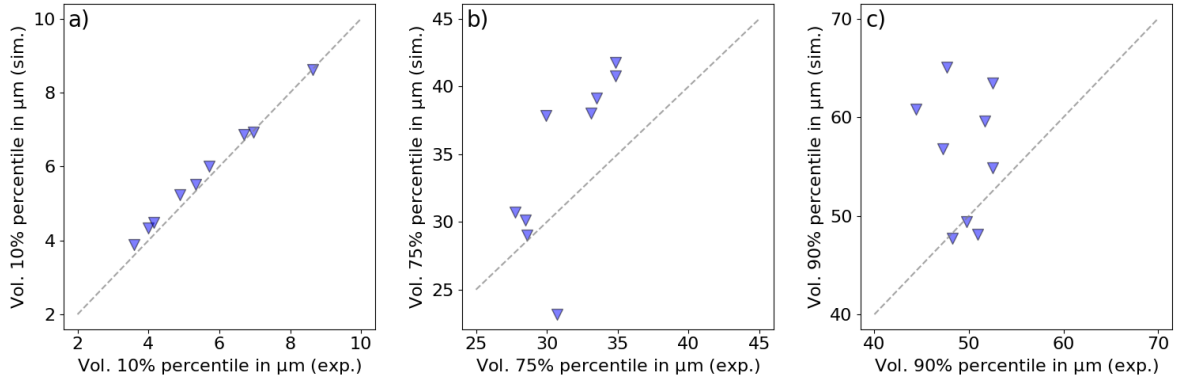

Figure **4**. Comparison of predicted volumetric 10 and 90 percentile with given C_3

Simulation results for D_{v10} are in good agreement with experimental results. Simulations are within 1 µm of absolute experimental values. Results for D_{v75} and D_{v90} are further scattered

with an absolute deviation from the experimental values of up to 7.9 µm and 15 µm. The average standard deviation of the experimental D_{v10} and D_{v90} is 0.6 µm and 2.0 µm, respectively. Exemplary experimental, log-normal and simplified MEG model predicted droplet-size distributions are presented in Figure **5**.

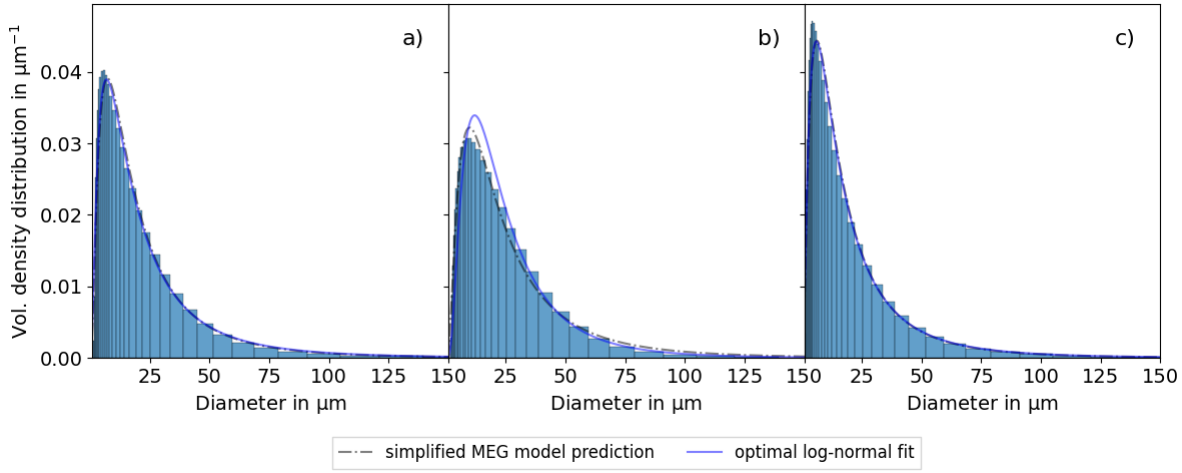

Figure **5**. Comparison of experimental and predicted droplet-size density functions for varying process parameters. For experiments a), b) and c) the volumetric flow-rate was 4, 6.34 and 6.34 mL/min and atomization pressure were 2.6, 1.6 and 3.4 bar, respectively.

Predictions of the simplified MEG model as seen in Figure 5 show good agreement with experimental data and are comparable with fitted log-normal distributions. Regarding the curve progressions two effects might cause the reduced predictive quality of D_{v90}. First, the assumed log-normal distribution might not be a perfect fit to the droplet-size distribution. Second, for higher percentiles small changes in the percentile tend to cause a greater change in droplet size.

Conclusions

The concept of combining predictive models for single droplet size, log-normal distribution and the MEG model is feasible. Predictions of the droplet-size distribution depend on accurate predictions of the Sauter-mean diameter. Predictions of Sauter-mean diameter by the calibrated Aliseda model deviate from experimental values. These deviations might be caused by deviations in the atomization pressure and measurement uncertainties. Further investigations into a more precise prediction of Sauter-mean diameter are required.

By postulating a log-normal distribution to the MEG model, its computational cost is significantly reduced. A constrained optimization is no longer required, and the number of optimization variables is reduced to the distribution parameter of the log-normal distribution. Predictions of the volumetric 10% percentiles deviate by approximately 1 µm form the optimal result. However, predictions for the 90% percentiles deviate significantly stronger from the optimal results. This might be explained by two reasons. First, the log-normal distribution is not capable of fully characterize the true droplet-size distribution. Second, deviations from the true distribution cause greater deviations at higher percentiles.

Predictive quality of the droplet-size distribution model depends on C_3. This calibration parameter however fluctuates and must be fitted separately for each experiment. Additional work into correlating this parameter process parameters must be conducted. A final model

would be beneficial for large sensitivity studies and the localization of optimal process parameters.

Nomenclature

a	specific surface area $(\mathrm{m^2\ kg^{-1}})$
b_g	boundary layer thickness (mm)
$\dot{m}$	mass flow rate $(\mathrm{kg\ s^{-1}})$
m_r	mass-flux ratio $(-)$
s	specific entropy liquid $(\mathrm{J\ kg^{-1}\ K^{-1}})$
p_{atom}	atomization pressure (bar)
p_1	pressure at nozzle exit (Pa)
x_{crit}	critical distance from nozzle (m)
$z_{r,x}$	z factor $(-)$
C_i	calibration parameter $(-)$
$D_{r,0}$	mean diameter $(\mu\mathrm{m})$
$D_{3,2}$	droplet Sauter-mean diameter $(\mu\mathrm{m})$
$D_{g,in}$	diameter inner edge ring gap $(\mu\mathrm{m})$
$D_{g,out}$	diameter outer edge ring gap (mm)
D_l	diameter liquid orifice (mm)
D_{v10}	volumetric 10% percentile $(\mu\mathrm{m})$
D_{v90}	volumetric 90% percentile $(\mu\mathrm{m})$
H_{sh}	Shannon entropy $(-)$
K	MEF parameter $(\mathrm{m^2\ kg\ s^{-2}\ K^{-1}})$
$\dot{N}_T$	droplet generation rate $(\mathrm{s^{-1}})$
Oh	Ohnesorge number $(-)$
P_r	probability density distribution $(-)$
$P_{r,LaG}$	lagrangian form distribution $(-)$
$P_{r,Log}$	log-normal distribution $(-)$
Re	Reynolds number $(-)$
T	temperature (K)
U	velocity at nozzle exit $(\mathrm{m\ s^{-1}})$
$\dot{V}$	volumetric flow rate $(\mathrm{mL\ min^{-1}})$
We	Weber number $(-)$
α_i	lagrangian fitting parameters $(-)$
η	viscosity $(\mathrm{Pa\ s})$
κ_T	Isothermal compressibility $(\mathrm{Pa^{-1}})$
$\bar{\mu}_{ln}$	log-normal location parameter $(-)$
ρ	density $(\mathrm{kg\ m^{-3}})$
σ_{ln}	log-normal distribution parameter $(-)$
σ_{ST}	surface tension $(\mathrm{N\ m^{-1}})$

Indices

$\bar{}$	normalized variables
g	atomization gas phase
gen	generated
l	liquid phase
r	distribution type

References

[1] Lister, J., Ennis, B., and Liu, L., 2004, The Science and Engineering of Granulation Processes.
[2] Razmi, R., Jubaer, H., Krempski-Smejda, M., Jaskulski, M., Xiao, J., Chen, X. D., and Woo, M. W., 2021, "Recent initiatives in effective modeling of spray drying," Drying Technology, 39(11), pp. 1614-1647.
[3] Kemp, I. C., Hartwig, T., Herdman, R., Hamilton, P., Bisten, A., and Bermingham, S., 2015, "Spray drying with a two-fluid nozzle to produce fine particles: Atomization, scale-up, and modeling," Drying Technology, 34(10), pp. 1243-1252.
[4] Chen, W., Chang, S.-Y., Kiang, S., Early, W., Paruchuri, S., and Desai, D., 2008, "The Measurement of Spray Quality for Pan Coating Processes," Journal of Pharmaceutical Innovation, 3(1), pp. 3-14.
[5] Masters, K., 1991, Spray Drying Handbook, Longman Scientific & Technical.
[6] Aliseda, A., Hopfinger, E. J., Lasheras, J. C., Kremer, D. M., Berchielli, A., and Connolly, E. K., 2008, "Atomization of viscous and non-newtonian liquids by a coaxial, high-speed gas jet. Experiments and droplet size modeling," International Journal of Multiphase Flow, 34(2), pp. 161-175.
[7] Ashgriz, N., 2011, Handbook of Atomization and Sprays: Theory and Applications.
[8] Ahmadi, M., and Sellens, R. W., 1993, "A Simplified Maximum-Entropy-Based Drop Size Distribution," Atomization and Sprays, 3(3), pp. 291-310.
[9] Li, X., Li, M., and Fu, H., 2005, "Modeling the Initial Droplet Size Distribution in Sprays Based on the Maximization of Entropy Generation," Atomization and Sprays, 15(3), pp. 295-322.
[10] Li, X., and Li, M., 2003, "Droplet Size Distribution in Sprays Based on Maximization of Entropy Generation," Entropy, 5(5), pp. 417-431.
[11] Niblett, D., Porter, S., Reynolds, G., Morgan, T., Greenamoyer, J., Hach, R., Sido, S., Karan, K., and Gabbott, I., 2017, "Development and evaluation of a dimensionless mechanistic pan coating model for the prediction of coated tablet appearance," International Journal of Pharmaceutics, 528(1-2), pp. 180-201.
[12] Lasheras, J. C., Villermaux, E., and Hopfinger, E. J., 1998, "Break-up and atomization of a round water jet by a high-speed annular air jet," Journal of Fluid Mechanics, 357, pp. 351-379.
[13] Shannon, C. E., 1948, "A Mathematical Theory of Communication," Bell System Technical Journal, 27(3), pp. 379-423.
[14] Elliott, J. A. W., 2020, "Gibbsian Surface Thermodynamics," J Phys Chem B, 124(48), pp. 10859-10878.
[15] Alderliesten, M., 2016, "Mean Particle Diameters. Part VIII. Computer Program to Decompose Mixtures of (Truncated) Lognormal Particle Size Distributions Using Differential Evolution to Generate Starting Values for Nonlinear Least Squares," Particle & Particle Systems Characterization, 33(9), pp. 675-697.